

The Dynamic Response of Two Parallel Structures in Elastic Half Space under SH Waves

ZHOU Deliang, WENG Zhiyuan
Tongji University, Wuhan, China

Abstract

In this paper, a method called BEEET which combines boundary element with eigenfunction expansion technique is developed to analyze the dynamic response of two parallel structures with complex shapes embedded in semi-infinite elastic medium under SH waves.

A. The problem and its solution

Consider the subway structures shown in Fig.1, the structures are assumed to be infinite long, lying parallel to the ground surface, they are of the same cross-section and material. The medium is homogeneous and elastic. The structures are denoted by I and II respectively.

It's seen that the structures divide the half space into three regions: R1 including R^I and R^{II}, R2 and R3, as per BEEET, the eigenfunction expansion is applied to R3, boundary element to R2 and R1, the displacements and stresses on boundaries can be obtained by use of the continuity conditions of displacement and stress between regions. The displacement and stress at any point in the region can be obtained by use of the displacements and stresses on the concerned boundary.

1. The eigenfunction expansion in R3(Farfield)

The displacement at any point in R3 consists of free-field displacement and scattering one. The waves are supposed to originate in R3. The incident waves are the harmonic SH waves with unit amplitude, it can be expressed as follows:

$$w^{(i)} = \exp[ik(x^* \sin \gamma + y^* \cos \gamma)] \quad (1)$$

where γ is the incident angle(see Fig.1), k the wave number and time factor $e^{i\omega t}$ is left out.

For the half space with homogeneous medium and regular ground surface, the incident waves reflect on the ground surface($y^*=0$)

the reflection waves can be expressed as:

$$w^{(v)} = \exp[ik(x^* \sin \psi - y^* \cos \psi)] \quad (2)$$

The free-field displacement is

$$w^{(w)} = w^{(w)} + w^{(v)} = 2 \cos(ky^* \cos \psi) \exp(ika^* \sin \psi) \quad (3)$$

Through the coordinate transform $x^* = x$, $y^* = y - H$

$$w^{(w)} = 2 \cos[k(y-H) \cos \psi] \exp(ikx \sin \psi) \quad (4)$$

The scattering-field displacement satisfying Helmholtz equation, boundary conditions on $y^* = 0$ and radiation condition can be expressed as:

$$w^{(s)} = \sum_{n=-\infty}^{\infty} A_n [H_n(kr) e^{in\theta} + H_n(kR) e^{in\theta}] \quad (5)$$

where H_n is the first kind Hankel function of order n , the coordinates (Y, θ) and (R, θ) are shown in Fig.1, A_n are constants.

In numerical calculation, however, n is finite. Assuming the nodal number on boundary $r = R_b$ is N_b (even), Eq.(5) becomes

$$w^{(s)} = \sum_{n=-N_1}^{N_2} A_n [H_n(kr) e^{in\theta} + H_n(kR) e^{in\theta}] \quad (6)$$

where $N_1 = N_b/2 - 1$, $N_2 = N_b/2$, $n_1 = n + N_2$, in order to apply the stress and displacement conditions of continuity on boundary, a quantity $q = \frac{\partial w}{\partial n}$ is introduced, where n is the component of outward normal on boundary. For circular boundary, $q = \frac{\partial w}{\partial r}$.

Applying Eqs(4) and (6) to boundary Bc, we obtain the nodal displacements on Bc:

$$\{W\} = \{W^{(w)}\} + [K]\{a\} \quad (7)$$

with $\{a\} = [A_1, A_2, \dots, A_{N_b}]^T$ being the unknown constant, and $[K]$ the matrix (square) related to the nodal locations.

Similarly, applying $q = \frac{\partial w}{\partial r}$ to the nodal points on boundary Bc results in:

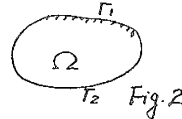
$$\{q\} = \{q^{(w)}\} + [M]\{a\} \quad (8)$$

where $[M]$ is also a square matrix related to the nodal location.

2. Boundary element in R2 and R1

Consider an arbitrary region Ω shown in Fig.2. According to weighted residual method, the displacement w satisfying Helmholtz equation $\nabla^2 W + k^2 W = 0$ in region Ω and the following boundary conditions:

$$\begin{aligned} w &= \bar{w} \text{ (prescribed) on } \Gamma_1 \\ q &= \bar{q} \text{ (prescribed) on } \Gamma_2 \end{aligned}$$



satisfies following equation

$$\int_{\Omega} (\nabla^2 W + k^2 W) w^* d\Omega = \int_{\Gamma_2} (q - \bar{q}) w^* d\Gamma - \int_{\Gamma_1} (w - \bar{w}) q^* d\Gamma \quad (9)$$

Integrating twice by parts results in

$$\int_{\Omega} (\nabla^2 w^* + k^2 w^*) w d\Omega = \int_{\Gamma} w^* q d\Gamma - \int_{\Gamma} q^* w d\Gamma \quad (10)$$

Let $\nabla^2 w^* + k^2 w^* + \delta_i = 0$ then, Eq.(10) becomes

$$c_i w_i + \int_{\Gamma} q^* w d\Gamma = \int_{\Gamma} q w^* d\Gamma \quad (11)$$

where c_i is a constant determined by the location of point i considered

$$c_i = \begin{cases} 1 & \text{inside} \\ 1/2 & \text{on smooth boundary} \\ 0 & \text{outside} \end{cases}$$

Discretization of boundary by constant element results in

$$\text{where } \sum_{j=1}^N H_{ij} W_j = \sum_{j=1}^N G_{ij} q_j \quad (12)$$

$$H_{ij} = \begin{cases} \bar{H}_{ij} + 1/2 & \text{if } i=j \\ \bar{H}_{ij} & \text{if } i \neq j \end{cases}$$

$$\bar{H}_{ij} = \int_{\Gamma} q^* d\Gamma_j, \quad G_{ij} = \int_{\Gamma} w^* d\Gamma_j$$

$i, j (i, j=1, \dots, N)$ is the nodal number on boundary Γ .

Applying Eq.(12) to R2 results in

$$\text{where } \begin{bmatrix} H_2^b & H_2^I & H_2^{II} \end{bmatrix} \begin{Bmatrix} W_2^b \\ W_2^I \\ W_2^{II} \end{Bmatrix} = \begin{bmatrix} G_2^b & G_2^I & G_2^{II} \end{bmatrix} \begin{Bmatrix} q_2^b \\ q_2^I \\ q_2^{II} \end{Bmatrix} \quad (13)$$

where $\{W_2^b\}$, $\{W_2^I\}$ and $\{W_2^{II}\}$ are the nodal displacements on boundary $r=R_b$, outer surfaces of structure I and II respectively, $\{q_2^b\}$, $\{q_2^I\}$ and $\{q_2^{II}\}$ are the corresponding stress quantities.

Applying Eq(12) to R1 results in:

For structure I:

$$\begin{bmatrix} H_1^I & H_1^O \end{bmatrix} \begin{Bmatrix} W_1^I \\ W_1^O \end{Bmatrix} = \begin{bmatrix} G_1^I & G_1^O \end{bmatrix} \begin{Bmatrix} q_1^I \\ q_1^O \end{Bmatrix} \quad (14)$$

where $\{W_1^I\}$, $\{W_1^O\}$ are displacements on inner and outer surfaces of structure I respectively, $\{q_1^I\}$, $\{q_1^O\}$ are the corresponding stress quantities. Similarly, for structure II,

$$\begin{bmatrix} H_1^{II} & H_1^O \end{bmatrix} \begin{Bmatrix} W_1^{II} \\ W_1^O \end{Bmatrix} = \begin{bmatrix} G_1^{II} & G_1^O \end{bmatrix} \begin{Bmatrix} q_1^{II} \\ q_1^O \end{Bmatrix} \quad (15)$$

where $\{W_1^{II}\}$, $\{W_1^O\}$ are displacements on inner and outer surfaces of structure II respectively, $\{q_1^{II}\}$, $\{q_1^O\}$ are the corresponding stress quantities. The boundary conditions are as follows:

$$\text{On the inner surfaces of structures: } \begin{cases} \{q_1^I\} = 0 \\ \{q_1^{II}\} = 0 \end{cases} \quad (16)$$

$$\text{On the outer surfaces of structures: } \begin{cases} \{W_1^O\} = \{W_1^O\} & \{W_1^O\} = \{W_1^O\} \\ \mu_1 \{q_1^O\} = -\mu_2 \{q_1^O\}, \mu_1 \{q_1^O\} = -\mu_2 \{q_1^O\} \end{cases} \quad (17)$$

$$\text{On the boundary } r=R_b: \begin{cases} \{W_2^b\} = \{W_2^b\} + [K]\{a\} \\ \mu_2 \{q_2^b\} = \mu_3 (\{q_2^b\} + [M]\{a\}) \end{cases} \quad (18)$$

Substituting Eqs (16-18) into Eqs(13-15) results in

$$\begin{bmatrix} H_1^I & H_1^O & -G_1^O & 0 & 0 & 0 & 0 \\ 0 & 0 & 0 & H_1^I & H_1^O & -G_1^O & 0 \\ 0 & H_2^b & \alpha_{12} G_2^b & 0 & H_2^I & \alpha_{12} G_2^I & D \end{bmatrix} \begin{Bmatrix} W_1^I \\ W_1^O \\ W_2^b \\ q_1^I \\ W_2^I \\ q_1^O \\ a \end{Bmatrix} = \begin{Bmatrix} 0 \\ 0 \\ 0 \\ 0 \\ 0 \\ P \end{Bmatrix} \quad (19)$$

$$\text{where } [D] = [H_2^b][K] - \alpha_{32} [G_2^b][M], \{P\} = \alpha_{32} [G_2^b]\{q_2^b\} - [H_2^b]\{W_2^b\}$$

$$\alpha_{12} = \mu_1/\mu_2, \quad \alpha_{32} = \mu_3/\mu_2, \quad \mu_i (i=1,2,3) \text{ are Lamé's constant for region } R_1, R_2 \text{ \& } R_3$$

The displacements and stress quantities on boundaries can be obtained by solving Eq(19).

B. Numerical results and discussion

There are some factors which have influences on the dynamic response of underground structure. In the previous studies^[1,2] on the dynamic response of single structure in half space, factors such as the physical properties of structure and surrounding medium, the wave type, wave frequency, incident angle, the

embedment depth of the structure have been considered. Undoubtedly, the factors mentioned above have influences on the dynamic response of double structures in half space. The effect by incident angle and wave frequency on dynamic problem of two parallel underground structures is taken into account.

In numerical calculation, the materials and their physical properties of structures and surrounding media are as follows: The materials of structures(R1) is concrete: ρ_c (density)= 2.24×10^3 KG/M³, μ_c (Poisson's ration)=0.2, E_c (Young's modulus)= 1.6×10^{10} N/M².

The material of R2 is soil: $\rho_s=2.665 \times 10^3$ KG/M³, $\mu_s=0.45$, $E_s=6.9 \times 10^8$ N/M².

The material of R3 is rock: $\rho_r=2.665 \times 10^3$ KG/M³, $\mu_r=0.25$, $E_r=7.567 \times 10^9$ N/M².

Other constant coefficients include: the embedment depth of structures, $H=20$ M, the distance between two structures, $2L=14$ M, $R_b=14$ M, $r_0=5.5$ M, $r_1=5$ M, $L_1=4$ M, $L_2=3$ M, $d=0.5$ M, k_1 , k_2 and k_3 are the wave numbers in R1, R2 and R3 respectively. The corresponding dimensionless quantities are $\xi_1=k_1 r_1$, $\xi_2=k_2 r_1$ and $\xi_3=k_3 r_1$ respectively.

The numerical results show the displacement amplitudes and stresses on boundaries due to various incident angles and frequencies. In the following content, the displacements and stresses on the outer surfaces of structures are called displacements and stresses respectively in short for convenience. It's seen from Fig.3 that $\psi=0^\circ$, the displacements on two structures are symmetrical to axis y, this is because both structures and load are symmetrical to axis y at $\psi=0^\circ$. At $\psi=90^\circ$, the displacements on both structures are larger than those on the corresponding structure at $\psi=0^\circ$, and displacements on the left structure are apparently larger than those on the right one. Also shown in the results is that as ψ increases between 0° and 90° , the displacements on the left structure increase faster than those on the right one. This may be explained as follows: when $0^\circ < \psi \leq 90^\circ$, the travelling waves encounter the left structure, at first, the waves reflect and scatter by the left structure, thus the right one gets less wave energy than the left one does. The left structure hides the transmission of wave energy to the right one.

In Fig.4, the dimensionless quantity $\xi_1=0.08162$, half the value of $\xi_1=0.16324$ in Fig.3. It's seen that, in this case, as ψ increases, the displacements increase very slowly, the obstruction of energy transmission caused by the left structure at $\psi=90^\circ$ is not apparent comparing with that in Fig.3.

By comparing Fig.3 and Fig.4, it's seen that at $\psi=0^\circ$, some nodal

displacements increase a bit as ϵ_1 decreases, while at $\gamma' = 90^\circ$, the displacements decrease sharply as ϵ_1 decreases.

Now, we consider the non-normalized stresses on the outer surfaces of structures. In antiplane strain case, the only non-zero stress is $\tau_{rz} = \mu \frac{\partial W}{\partial r}$ for outer surfaces of structures, $\tau_{rz} = \mu_1 \frac{\partial W}{\partial r}$, let $\tau_{rz}^* = \tau_{rz} / \beta$ with β being a constant of $0.1 \mu_1$.

It's seen from Fig.5 that the stresses, like the displacements in Fig.3 at $\gamma' = 0^\circ$, are symmetrical to axis y at $\gamma' = 0^\circ$. This is of the same reason as mentioned above. Also seen in Fig.5 is that as γ' increases, the stresses on upper and lower part of both structures decrease while those on the left and right side of structures increase. At $\gamma' = 90^\circ$, the stresses on right part of right structure are larger than those on the corresponding part of left structure, while the stresses on the left part of two structures are almost the same. Contrary to this, in Fig.3 at $\gamma' = 90^\circ$, the left part displacements of two structures are almost the same, while displacements on right part of left structure are larger than those on the corresponding part of right one. All these obey the energy principle, this also proves the numerical results are correct.

From Fig.6, it's seen the stresses are similar to those in Fig.5. Comparing Fig.5 and Fig.6, we can find that the stresses decrease greatly as ϵ_1 decreases. In Fig.6, it's found the stresses on right part of structures are almost the same while the stresses on left part of right structure are larger than those on the corresponding part of left one at $\gamma' = 90^\circ$. This is the difference from the stress distributions in Fig.5 at $\gamma' = 90^\circ$.

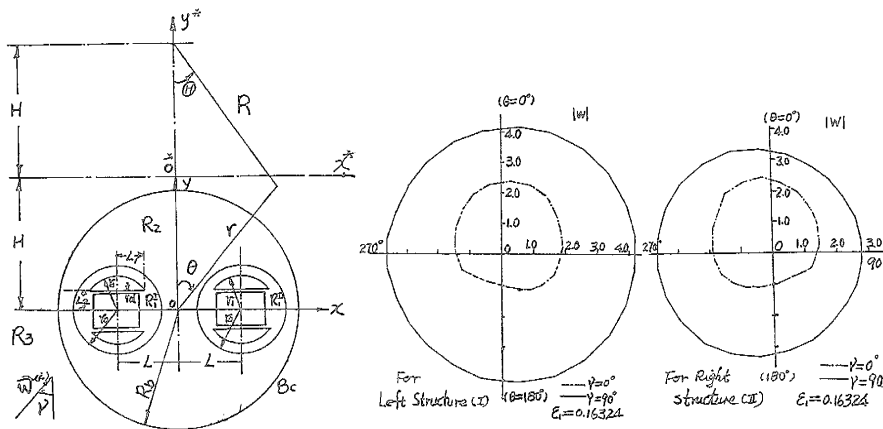


Fig.1 Geometry of the Problem

Fig. 3 Displacement amplitudes distribution on outer surfaces of structures at $\gamma = 0^\circ$ and $\gamma = 90^\circ$ when $\epsilon_1 = 0.16324$

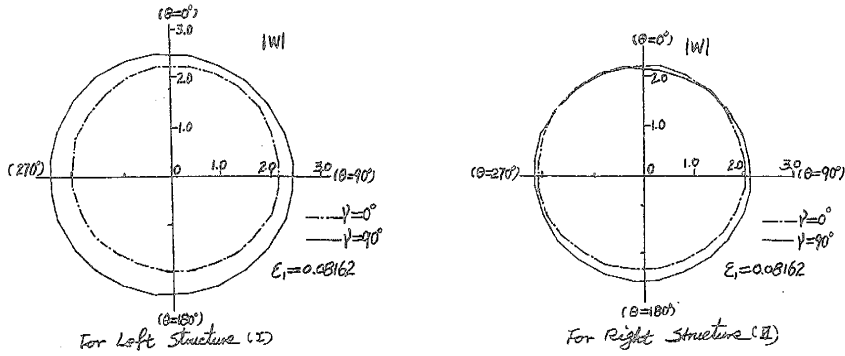


Fig.4 Displacement amplitudes distribution on outer surfaces of structures at $\psi=0^\circ$ and $\psi=90^\circ$ when $\epsilon_1=0.08162$

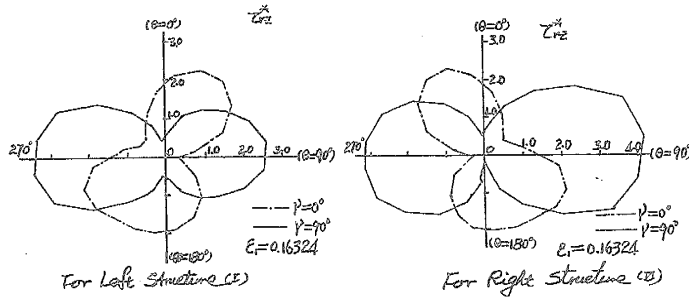


Fig.5 The normalized stresses distribution on outer surfaces of structures at $\psi=0^\circ$ and 90° when $\epsilon_1=0.16324$

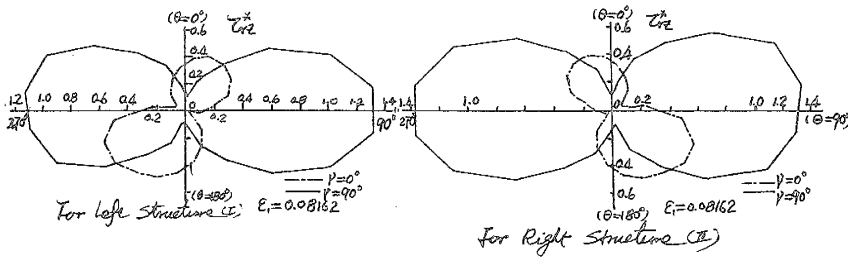


Fig.6 The normalized stresses distribution on outer surfaces of structures at $\psi=0^\circ$ and 90° when $\epsilon_1=0.08162$

Reference

1. Zhou Deliang, Weng Zhiyuan and Xu Bang Wer, 'The Analysis of Dynamic Response of Underground Structures', Proceedings of the 2nd China-Japan Symposium on Boundary Element Methods, PP.415-422, 1988.